

Synthesis of Formamidinium Lead Halide Perovskite Nanocrystals through Solid-Liquid-Solid Cation Exchange

K. Hills-Kimball,^a Y. Nagaoka,^a C. Cao,^a E. Chaykovsky,^a and O. Chen^{*a}

^a *Department of Chemistry, Brown University, Providence, Rhode Island 01912, United States*

*Email: ouchen@brown.edu

Chemicals

Lead bromide (PbBr₂, 99.999%), toluene (anhydrous, 98%), formamidinium acetate salt (FA(ac), 99%), mesitylene (98%), hydrobromic acid (48%), diethyl ether (>99.9%) and octylamine (99%) were purchased from Sigma Aldrich. Lead chloride (PbCl₂, 99.999%), lead iodide (PbI₂, 98.5%), hydrochloric acid (36% w/w), and oleic acid (90%) were purchased from Alfa Aesar. N,N-dimethylformamide (DMF) was purchased from Fisher Scientific. Methylammonium Iodide (MAI, >98%) was purchased from TCI. DMF was dried using sieves prior to use. All other chemicals were used as received without further purification.

Synthesis of MAX (X= Cl⁻, Br⁻)

Methylammonium bromide (MABr) and methylammonium chloride (MACl) were synthesized following a literature procedure.¹ 20 mL hydrobromic acid (48%) (or 8 mL hydrochloric acid) was added to 10 mL methylammonium (33 wt% in ethanol) at 0°C. The solution was kept stirring in an ice bath for 3.5 hours and then the solvent was removed by evaporation. The product was then washed three times with diethyl ether and dried under vacuum overnight.

Synthesis of MAPbX₃ Nanocrystals (X= Cl⁻, Br⁻, I⁻)

Hybrid organic-inorganic perovskite (HOIP) methylammonium lead bromide (MAPbBr₃) nanocrystals (NCs) were synthesized following a modified literature procedure.¹ 100 μL dried DMF was added to 10 mL anhydrous toluene, and the resulting solution was stirred under nitrogen. A precursor solution was made by combining 0.018 g (0.16 mmol) MABr with 0.0734 g (0.2 mmol) PbBr₂ in 5 mL DMF with 20 μL octylamine and 0.5 mL oleic acid. (Cl⁻ and I⁻ precursors were also made in a similar fashion using the same molar amounts of MAX and PbX₂ and

excluding addition of oleic acid in the case of the Cl⁻ precursor). 0.2 mL of the precursor solution was then quickly injected into the toluene/DMF solution, and stirring was immediately stopped. The solution reacted at room temperature for 2 minutes and was then cooled in an ice bath for 10 minutes. The reaction solution was allowed to sit overnight in order to separate precipitates from the NCs. MAPbX₃ particles with varying halide compositions (I⁻/Br⁻ and Cl⁻/Br⁻) were synthesized by combining desired amounts of halide precursor solutions prior to injection into the toluene/DMF solution.

FA⁺ Cation Exchange Reaction

0.2 g FA(ac) was added to 20 mL of the as-synthesized MAPbBr₃ perovskite NC colloidal solution. The exchange reaction was monitored using UV-vis and photoluminescence (PL) spectroscopy, and typically proceeded for 150 minutes before complete conversion to FAPbBr₃ was achieved. The resulting particles were separated from the FA(ac) solids by pipetting the upper solution and filtering through glass wool. N₂ was bubbled into the filtered solution for 10 minutes. Formamidinium (FA⁺) cation exchange reactions for the HOIP NCs with mixed halides followed a similar procedure with altered reaction times. Power X-ray diffraction (XRD) was used to confirm the completion of the cation exchange.

Measurements

UV-Vis absorption spectra were measured using an Agilent Technologies Cary 5000 UV-Vis-NIR Spectrophotometer. PL spectra were measured using an Edinburgh Instruments Fluorescence Spectrometer FS5. For all optical data, synthesized perovskite particles were diluted in anhydrous toluene.

Powder XRD data was obtained on a Bruker D8 Discovery 2D X-ray Diffractometer equipped with a Vantec 500 2D area detector (U= 40 kV, I= 40 mA, Cu K α , 1.541 nm radiation). Aliquots of perovskite NCs in toluene were added to an equal volume of mesitylene. This solution was dropped onto a glass slide, which was gently heated to remove the solvent. The XRD samples with mixed halide compositions were prepared by putting the colloidal solution into a glass vial along with a small piece of glass slide. Centrifugation was then used in order to form a NC film samples onto the glass slide.²

Transmission electron microscopy (TEM) measurements were performed on a JEOL 2100F operated at 200kV. The sample in a toluene solution (~10 μ L) was directly dropped onto a 300-mesh copper TEM grid and dried in ambient conditions. FT-IR measurements were performed on a Jasco FT-IR 4100. The NCs were collected through centrifugation and redispersed in a small amount of hexane. The concentrated sample was directly dropped onto a NaCl pellet for the FT-IR measurements.

PL lifetime measurements were performed on an Edinburgh Instruments Fluorescence Spectrometer FS5-TCSPC with an EPLED-360 light source. PL QY measurements were performed on an Edinburgh Instruments Fluorescence Spectrometer equipped with an integrating sphere.

Calculations for halide composition determination and expected XRD peak shift in mixed halide HIOP NCs

Halide composition in $\text{MAPbBr}_x\text{X}_{3-x}$ ($X = \text{Cl}^-$ or I^-) was calculated using Vegard's law. Expected change in lattice constant upon complete conversion to $\text{FAPbBr}_x\text{X}_{3-x}$ was also calculated using Vegard's Law, and results were compared to measured lattice constants for final FA samples.³⁻⁶

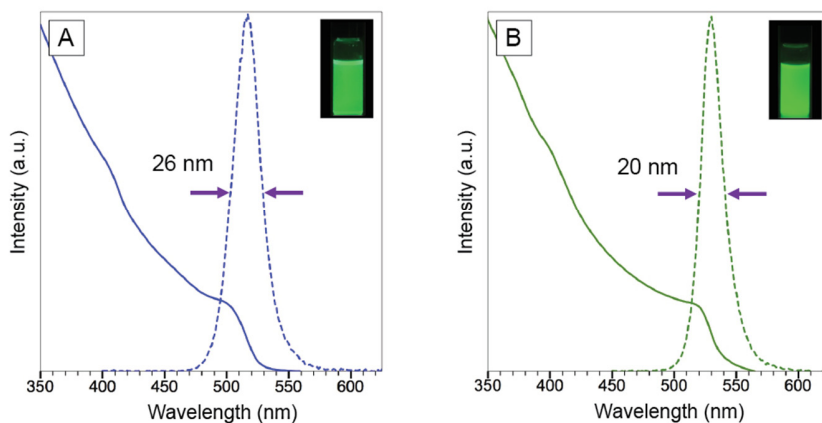


Figure S1. (A) Absorption (solid line) and PL emission (dotted line) spectra of starting MAPbBr₃ nanocrystals showing an emission peak centered at 515 nm with a full width at half maximum (FWHM) of 26 nm. Inset shows a photograph of the MAPbBr₃ perovskite nanocrystals in anhydrous toluene under UV illumination. (B) Absorption (solid line) and PL emission (dotted line) spectra of FAPbBr₃ nanocrystals showing an emission peak centered at 531 nm with a narrow FWHM of 20 nm. Inset shows a photograph of the FAPbBr₃ perovskite nanocrystals in anhydrous toluene under UV illumination.

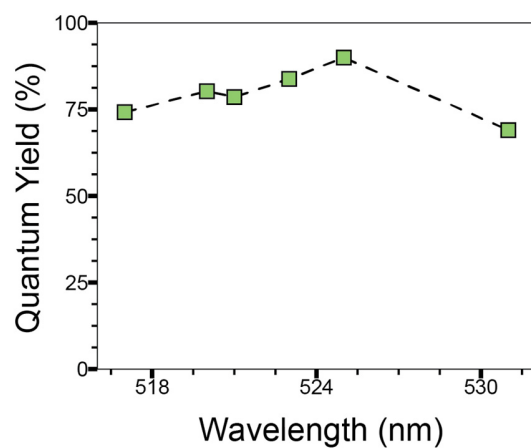


Figure S2. Evolution of photoluminescence quantum yield during the FA^+ exchange reaction. Initial MAPbBr_3 and final FAPbBr_3 nanocrystals were measured using the integrating sphere.

Table S1. Lifetime fitting results for FA⁺ cation exchange reaction (spectra shown in Figure 1D).

	515 nm		520 nm		524 nm		527 nm		531 nm	
	Value (ns)	Relative (%)								
τ_1	8.3	93	7.8	80	6.8	71	5.9	65	4.4	52
τ_2	35.5	7	31.9	20	41.2	29	53.7	35	69.9	48
τ_{average} (ns)	10.2		12.7		16.9		22.7		35.9	

Table S2. Evolution of the lattice constant in the hybrid organic-inorganic perovskite nanocrystals over the course of the FA⁺ cation exchange reaction (full spectra shown in Figure 2A).

	517 nm		524 nm		526 nm		531 nm	
	Peak Position (°)	d-spacing (Å)	Peak Position (°)	d-spacing (Å)	Peak Position (°)	d-spacing (Å)	Peak Position (°)	d-spacing (Å)
(100)	15.02	5.89	14.90	5.94	14.76	6.00	14.62	6.05
(110)	21.32	4.16	20.96	4.23	21.06	4.22	20.92	4.24
(200)	30.14	2.96	30.08	2.97	29.94	2.98	29.64	3.01
(210)	33.82	2.65	33.68	2.66	33.50	2.67	33.28	2.69
(211)	37.20	2.42	36.96	2.43	36.90	2.43	36.68	2.45
(220)	43.20	2.09	43.08	2.10	42.64	2.12	42.56	2.12
(300)	45.96	1.97	45.85	1.98	45.54	1.99	45.22	2.00
Lattice Constant (Å)	5.91(±0.02)		5.95 (±0.02)		5.97(±0.01)		6.01(±0.02)	

Table S3. FTIR peak assignments for MAPbBr₃ and FAPbBr₃ particles (full spectra shown in Figure 3A).⁷⁻⁸

	Peak (cm ⁻¹)	Intensity	Assignment
MAPbBr ₃	3189	strong	NH ₃ symmetric stretch
	3148	strong	NH ₃ symmetric stretch
	3042	shoulder	NH ₃ symmetric stretch
	1472	strong	NH ₃ asymmetric bend
FAPbBr ₃	3407	medium	NH ₂ symmetric stretch
	3359	weak	NH ₂ symmetric stretch
	3272	medium	NH ₂ symmetric stretch
	3171	weak	NH ₂ symmetric stretch
	1712	strong	C=N symmetric stretch

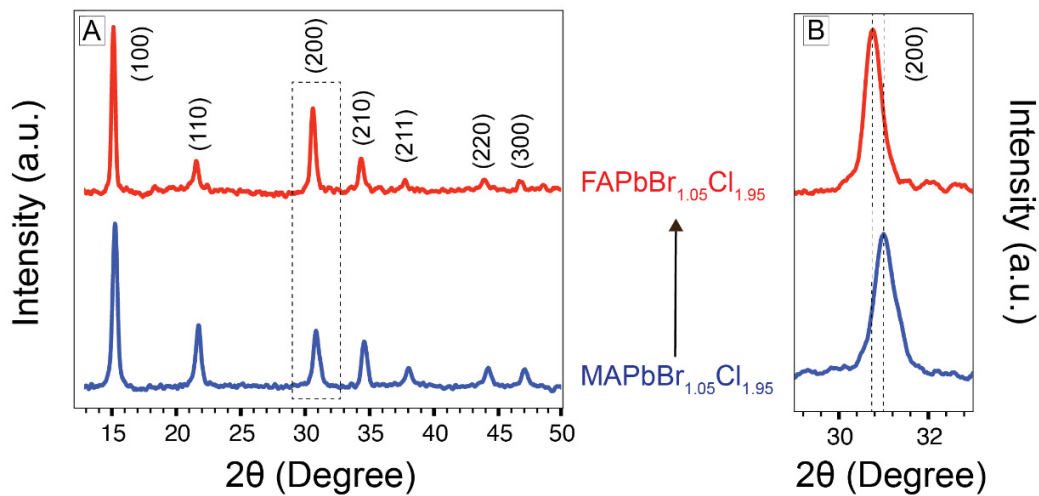


Figure S3. (A) XRD spectra of starting $\text{MAPbBr}_{1.05}\text{Cl}_{1.95}$ nanocrystals (blue) and final $\text{FAPbBr}_{1.05}\text{Cl}_{1.95}$ nanocrystals (red) following the completion of the cation exchange. (B) Zoomed in XRD spectra of rectangular area labelled in (A) for clear visualization of (200) peak shifting.

Table S4. Change in lattice constant in the chloride containing HOIP NCs upon exchange of MA^+ with FA^+ (full XRD spectra shown in Figure S3). Expected lattice constant of 5.82\AA for final $\text{FAPbBr}_{1.05}\text{Cl}_{1.95}$ nanocrystals was calculated using Vegard's Law.³⁻⁶

	Initial		Final	
	Peak Position ($^{\circ}$)	d-spacing (\AA)	Peak Position ($^{\circ}$)	d-spacing (\AA)
(100)	15.42	5.75	15.26	5.80
(110)	21.90	4.06	21.70	4.10
(200)	31.01	2.88	30.76	2.91
(210)	34.74	2.58	34.48	2.60
(211)	38.21	2.36	37.89	2.37
(220)	44.36	2.04	44.02	2.06
(300)	47.21	1.93	46.85	1.94
Lattice Constant (\AA)	5.76 (\pm 0.01)		5.81 (\pm 0.01)	

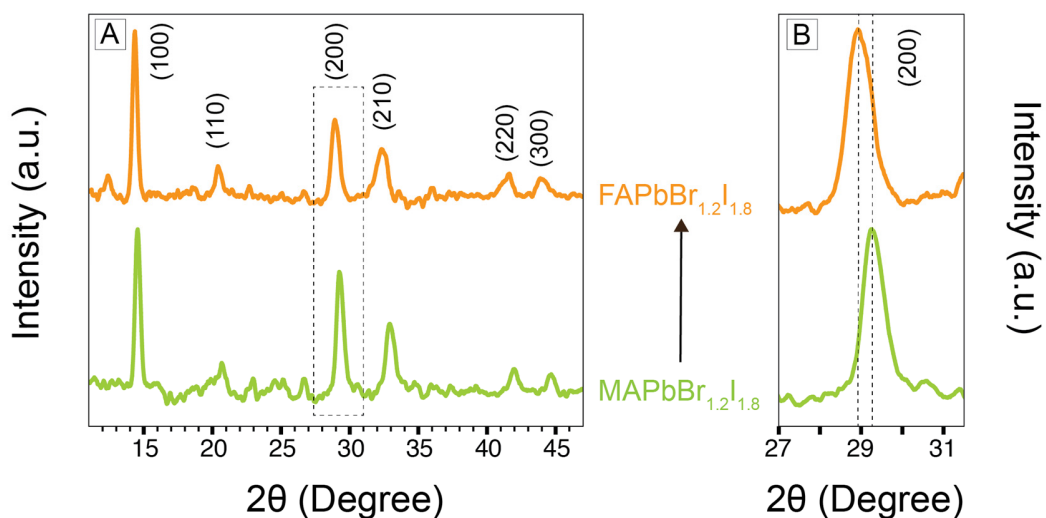


Figure S4. (A) XRD spectra of starting MAPbBr_{1.2}I_{1.8} nanocrystals (green) and final FAPbBr_{1.2}I_{1.8} nanocrystals (orange) following the completion of the cation exchange. (B) Zoomed in XRD spectra of rectangular area labelled in (A) for clear visualization of (200) peak shifting.

Table S5. Change in lattice constant in the iodide containing HOIP NCs upon exchange of MA with FA (full XRD spectra shown in Figure S4). Expected lattice constant of 6.16 Å for final FAPbBr_{1.2}I_{1.8} nanocrystals was calculated using Vegard's Law.³⁻⁶

	Initial		Final	
	Peak Position (°)	d-spacing (Å)	Peak Position (°)	d-spacing (Å)
(100)	14.56	6.08	14.36	6.17
(110)	20.70	4.29	20.40	4.35
(200)	29.26	3.05	28.92	3.09
(210)	32.90	2.72	32.32	2.77
(220)	42.00	2.15	41.62	2.17
(300)	44.68	2.03	43.90	2.06
Lattice Constant (Å)	6.08 (± 0.01)		6.17 (± 0.02)	

References

- 1 Zhang, F. et al. Brightly luminescent and color-tunable colloidal CH₃NH₃PbX₃ (X= Br, I, Cl) quantum dots: potential alternatives for display technology. *ACS nano* **9**, 4533-4542 (2015).
- 2 Kim, Y., Yassitepe, E., Voznyy O., Comin R., Walters G., Gong X., Kanjanaboos P., Nogueira A.F., & Sargent, E. H. Efficient luminescence from perovskite quantum dot solids. *ACS Applied Materials & Interfaces* **7**, 25007-25013 (2015).
- 3 West, A. R. *Solid state chemistry and its applications*. (John Wiley & Sons, 2007).
- 4 Zhong, X., Feng, Y., Knoll, W. & Han, M. Alloyed Zn_x Cd_{1-x} S Nanocrystals with Highly Narrow Luminescence Spectral Width. *Journal of the American Chemical Society* **125**, 13559-13563 (2003).
- 5 Chiu, H.-K., Chiang, I.-C. & Chen, D.-H. Synthesis of NiAu alloy and core-shell nanoparticles in water-in-oil microemulsions. *Journal of Nanoparticle Research* **11**, 1137-1144 (2009).
- 6 Sun, D. *et al.* Biogenic flower-shaped Au-Pd nanoparticles: synthesis, SERS detection and catalysis towards benzyl alcohol oxidation. *Journal of Materials Chemistry A* **2**, 1767-1773 (2014)
- 7 Zhou, Z., Pang, S., Ji, F., Zhang, B. & Cui, G. The fabrication of formamidinium lead iodide perovskite thin films via organic cation exchange. *Chemical Communications* **52**, 3828-3831 (2016).
- 8 Xie, L. Q. *et al.* Organic-inorganic interactions of single crystalline organolead halide perovskites studied by Raman spectroscopy. *Phys Chem Chem Phys* **18**, 18112-18118, doi:10.1039/c6cp01723a (2016).